On-surface synthesis of a two-dimensional porous coordination network: Unraveling adsorbate interactions

Manfred Matena,[1,2,*] Jonas Björk,[3,4,*] Markus Wahl,[1] Tien-Lin Lee,[5,†] Jörg Zegenhagen,[5] Lutz H. Gade,[6] Thomas A. Jung,[1,7] Mats Persson,[4,8] and Meike Stöhr[1,9,‡]

[1]*Department of Physics, University of Basel, Klingelbergstrasse 82, 4056 Basel, Switzerland*
[2]*Donostia International Physics Center, Paseo Manuel Lardizabal 4, 20018 San Sebastian, Spain*
[3]*Department of Physics, Chemistry and Biology, IFM, Linköping University, 58183 Linköping, Sweden*
[4]*Surface Science Research Centre, Department of Chemistry, University of Liverpool, Liverpool, United Kingdom*
[5]*European Synchrotron Radiation Facility, 38043 Grenoble, Cedex 9, France*
[6]*Anorganisch-Chemisches Institut, Universität Heidelberg, Im Neuenheimer Feld 270, 69120 Heidelberg, Germany*
[7]*Laboratory for Micro- and Nanotechnology, Paul-Scherrer-Institute, 5232 Villigen, Switzerland*
[8]*Department of Applied Physics, Chalmers University of Technology, 41296 Gothenburg, Sweden*
[9]*Zernike Institute for Advanced Materials, University of Groningen, Nijenborgh 4, 9747 AG Groningen, The Netherlands*

(Received 16 July 2014; published 5 September 2014)

We present a detailed experimental and theoretical characterization of the adsorption of the perylene derivative 4,9-diaminoperylene-quinone-3,10-diimine (DPDI) on Cu(111) and compare it to its threefold dehydrogenated derivative 3deh-DPDI, which forms in a surface reaction upon annealing. While DPDI itself does not give rise to long-range ordered structures due to lack of appropriate functional groups, 3deh-DPDI acts as an exoligand in a Cu-coordinated honeycomb network on Cu(111). The main focus of this work lies on the analysis of intermolecular and molecule-substrate interactions by combining results from scanning tunneling microscopy, x-ray photoelectron spectroscopy, x-ray standing wave measurements, and density functional theory. We show, in particular, that the interactions between metal atoms and organic ligands effectively weaken the molecule-surface interactions for 3deh-DPDI leading to an increase in molecule-substrate distances compared to the DPDI precursor. Our experimental findings also shed light on the applicability of current theories, namely van der Waals corrections to density functional theory.

DOI: 10.1103/PhysRevB.90.125408 PACS number(s): 68.37.Ef, 68.43.Fg, 68.49.Uv, 71.15.Mb

I. INTRODUCTION

Research on metal-organic frameworks (MOFs) has grown rapidly over the past 1.5 decades, as they represent functional ultrahigh surface area materials with a wide range of possible applications, such as gas storage, catalysis, and chemical separation [1–4]. Thin film MOFs, the limiting case being two-dimensional (2D) surface MOFs [5–7], offer the prospect of functionalizing surfaces and interfaces in a highly ordered fashion which may lead to significant changes in their optical, electronic, or tribological properties. Two-dimensional surface MOFs are composed of metal centers linking organic molecules (ligands), where the metal atoms are either coadsorbed with the molecules or generated intrinsically from the metal substrate. In this way, well-defined molecular nanostructures can be created on surfaces, which are mainly controlled by the choice of molecular precursors and metal atoms. Furthermore, the substrate may not only function as a support reducing the dimensionality of the system, but may also interact chemically with the adsorbed molecules and even induce chemical reactions resulting in molecular building blocks that otherwise cannot be stabilized through classical chemical synthesis.

Despite the comprehensive literature on 2D MOFs [5–14], there are still fundamental issues that have been barely addressed so far. In particular, experimental studies on the molecule-substrate bonding distances, which provide the points of reference for adequate theoretical modeling, are rare—in contrast to the numerous experimental studies on single molecule adsorption [15,16] and 2D molecular layers based on intermolecular interactions different than metal coordination [17–26]. However, these data are crucial for understanding molecule-substrate interactions and of interest for determining possible distortions from the planar geometry of surface-confined 2D MOFs.

So far, only a few theoretical studies using density functional theory (DFT) have investigated molecule-substrate bonding distances for 2D MOFs in detail [27–29]. Notably, nonlocal van der Waals (vdW) interactions play a fundamental role in the adsorption of large molecules on surfaces [30] and these interactions are particularly challenging for the theoretical modeling by DFT. A generally applicable theoretical method to model molecular adsorption, especially on metals, remains elusive [17,31]. Reliable adsorption heights of molecules in 2D MOFs are therefore mainly accessible from experimental data, at current, while these are essential to advance DFT and other theoretical tools.

Two different approaches to correct for vdW interactions in DFT have emerged. The first introduces an additive atom pairwise potential of the form C_6R^{-6}, where C_6 is an

*These authors contributed equally.
†Present address: Diamond Light Source Ltd, Harwell Science and Innovation Campus, Didcot, Oxfordshire, OX11 0DE, United Kingdom.
‡Corresponding author: m.a.stohr@rug.nl

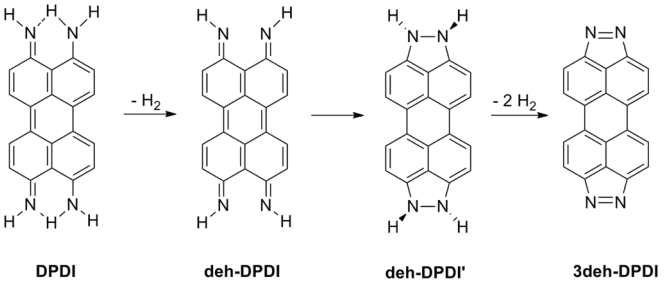

FIG. 1. Thermally induced dehydrogenation of DPDI on a metal surface via the quinoidal bisimino form deh-DPDI and further cyclization and dehydrogenation resulting in the triply dehydrogenated 3deh-DPDI that acts as an exoligand in the formation of the surface MOF discussed in this work.

atom-specific parameter determining the interaction strength and R is the distance between the two atoms [32–34]. The dispersion-corrected (DFT-D) methods are particularly difficult for metal surfaces due to difficulties in describing the polarizability of a metal. Notably, this problem was addressed with the DFT + vdW^{surf} method [34], with promising results [35]. Furthermore, recently it was demonstrated how $C3$ and $C5$ parameters can be calculated for atoms on surfaces [36], but which remain to be applied for molecular adsorption. The second approach is based on treating the vdW interactions by a truly nonlocal density functional. The so-called van der Waals density functional (vdWDF) [37] was designed to work seamlessly for both large and small separations, thus avoiding the problem of the damping function. However, it has been established that the original form of the vdWDF gives too large adsorption distances [38], while a number of modifications have been proposed [39–42].

Here we present detailed three-dimensional structural information of a surface-confined 2D MOF using the perylene derivative 4,9-diaminoperylene-quinone-3,10-diimine (DPDI) on Cu(111) as a model system. At elevated temperatures DPDI has been shown very recently to eliminate three molecules of H_2 to give 3deh-DPDI (Fig. 1), which interacts with Cu adatoms to form a highly ordered nanoporous network [43]. Difficulties in detecting the coordinated copper adatoms by STM had led us to suggest in an earlier study that the transformation of DPDI stopped at the monodehydrogenated diimine species deh-DPDI which was thought to aggregate via resonance-assisted H bonding between the molecules to form the network [44].

However, the extraordinary high stability of the network led us to re-investigate the surface transformations of DPDI. Based on a combination of STM and near edge x-ray absorption fine structure data as well as a re-investigation and re-interpretation of the N1s x-ray photoemission spectroscopy (XPS) signatures, backed up by DFT modeling, we put forward a structural model in which the 3deh-DPDI acts as a bridging exoligand within a surface coordination network [43]. To obtain detailed information about the lateral configuration of the surface-confined 2D MOF, a combination of scanning tunneling microscopy (STM), XPS, and x-ray standing wave (XSW) measurements have been carried out, and the system has been analyzed by extensive DFT modeling. The XSW data, in particular, provide insight into the vertical bonding distances of the 2D MOF, and this type of information allowed us to investigate the role of vdW corrections in the DFT modeling of such surface structures.

II. EXPERIMENT

A. Sample preparation

All experiments were performed under ultrahigh vacuum (UHV) conditions (base pressure of 10^{-10} mbar). The (111)-oriented Cu single crystal was prepared by subsequent cycles of sputtering with Ar^+ ions and annealing at approximately 500 °C. The molecules were deposited onto the Cu surface from a glass crucible that was heated inside a commercial evaporator (Kentax GmbH). The rate was controlled by a quartz crystal microbalance.

B. Scanning tunneling microscopy

The STM images were taken at low temperature (either 77 or 5 K) with a commercial low temperature STM (Omicron NanoTechnology GmbH) which was operated by the Nanonis SPM control system (Specs GmbH). The bias voltage was applied to the tip. However, the bias voltages given in the paper refer to a grounded tip. The software WSxM was used for data processing of the STM images [45].

C. X-ray photoelectron spectroscopy and x-ray standing wave experiments

XSW and XPS measurements were performed at beamline ID32 at the European Synchrotron Radiation Facility (ESRF) in Grenoble. Spectra were recorded in normal incidence geometry, i.e., the sample surface was mounted perpendicular to the incoming x-ray beam. The hemispherical analyzer (Physical Electronics) was mounted at an angle of 45° with respect to the incoming x-ray beam. In the XSW measurements, the photon energy was scanned in small steps over the Bragg condition for Cu(111) (around 2.97 keV) and XPS spectra were recorded for each photon energy. The XPS measurements (Fig. 2) for the nonannealed sample were done at a photon energy of 2.958 keV, whereas the photon energy was 2.964 keV for the spectra taken after annealing. All spectra were taken at room temperature. For the determination of the coherent fractions and positions, the program DARE developed by J. Zegenhagen was used. The nondipolar parameters were taken from Ref. [18].

D. Density functional theory modeling

Periodic density functional theory calculations were carried out with the VASP code [46], with the ion-core interactions described by the projected augmented wave (PAW) method [47,48]. Semilocal DFT calculations were performed with the PW91 functional [49]. Calculations with the van der Waals density functional (vdWDF) [37] were carried out using the original approach with revPBE exchange (revPBE-vdWDF) [50], as well as the PBE (PBE-vdWDF) [51] and optB86b (optB86b-vdWDF) [39] exchange, as indicated in the text. Furthermore, calculations with the Grimme correction (DFT-D2) [32] on the PBE functional were carried out. For the

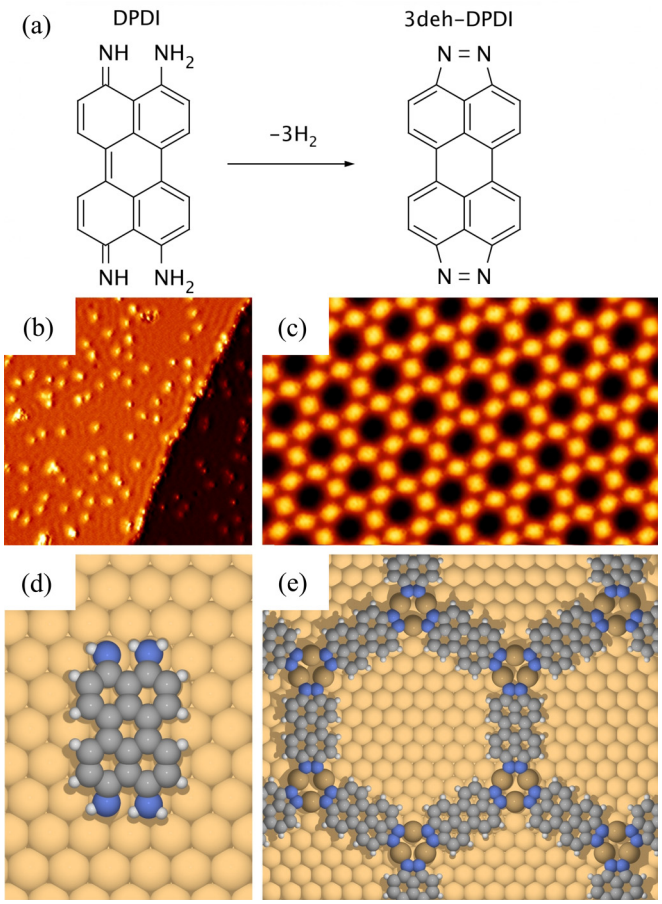

FIG. 2. (Color online) (a) Chemical transformation of DPDI upon annealing at 200 °C on Cu(111) into its dehydrogenated derivative 3deh-DPDI. (b) STM image (50 × 50 nm^2, 5 K) for submonolayer coverage of DPDI adsorbed on Cu(111) held at room temperature. The molecules stay isolated and do not form any ordered structure. (d) DFT calculations show that single DPDI molecules adsorb preferably with their perylene core centered above a bridge position and with each nitrogen atom on top of a surface atom. (c) STM image (18 × 11 nm^2, 77 K) for submonolayer coverage of DPDI adsorbed on Cu(111) after annealing at 200 °C. The molecules arrange in a porous network. (e) Tentative molecular model for the porous 3deh-DPDI network formed by incorporation of three adatoms in each vertex where they interact with the N functionalities of three 3deh-DPDI molecules. The adatoms are illustrated darker than the surface atoms.

DFT-D2 calculations, vdW corrections between Cu atoms were not included, and for the molecule-surface interactions only the surface atoms in the outermost surface layer were considered as proposed by McNellis and co-workers [52].

In all calculations the plane waves were expanded to a cutoff of 400 eV and the Γ point was used to sample the first Brillouin zone. For the calculations of isolated DPDI molecules a $p(7 \times 9)$ unit cell was used, while for the network a $p(10 \times 10)$ unit cell was used, as previously determined from LEED experiments [44]. The Cu(111) surface was modeled by four layered slabs. All structures were structurally optimized until the forces on the atoms in the adsorbate and the two outermost layers of the slab were smaller than 0.01 eV/Å. STM images were calculated using the Tersoff-Hamann approximation [53] as implemented by Lorente and Persson [54].

III. RESULTS AND DISCUSSION

A. Preparation of the 2D MOF

In a first step, DPDI molecules [Fig. 2(a)] were deposited on the Cu(111) surface held at room temperature. For molecular coverages below one monolayer (ML) [55], the molecules were found to be mobile on the Cu surface [44]. This molecular mobility was frozen when the sample temperature was lowered to 5 K and individual molecules could be identified in STM images [Fig. 2(b)]. However, no ordered structure was formed, which we attribute to the fact that the molecules cannot develop any attractive intermolecular interactions besides weak vdW interactions. Upon annealing at 200 °C and for coverages below 0.73 ML, a porous network was formed [Fig. 2(c)]. As will be demonstrated in more detail below, the molecules in the mobile phase are intact, whereas for the formation of the metal-coordinated porous network the DPDI molecules underwent a chemical transformation: the nitrogen atoms of DPDI were completely dehydrogenated and an azo bridge formed between adjacent nitrogen atoms [3deh-DPDI, see Fig. 2(a)]. It should be noted that while the isosteric hydrocarbon, dicyclopenta(1,2,3-cd:1′,2′,3′-lm)perylene, has been known for some time [56], the synthesis and isolation of its tetraaza-analog 3deh-DPDI has not been successful to date, probably due to its highly reactive nature. Nevertheless, on the Cu surface 3deh-DPDI is stabilized by metal coordination to Cu adatoms, which were generated by the annealing process [57]. Within this 2D MOF, each Cu adatom is coordinated to two nitrogen atoms of two adjacent molecules, resulting in an adatom-to-molecule ratio of 2:1.

B. Properties of the mobile phase vs the 2D MOF

Information on the adsorption geometry of the mobile phase of DPDI on Cu(111) was obtained by DFT calculations of the isolated adsorbed molecules. It turned out that the most stable adsorption position for DPDI has the central phenyl ring adsorbed on a bridge position [Fig. 2(d)]. The most stable structure for the porous network involving the 3deh-DPDI molecules obtained from DFT is shown in Fig. 2(e). The MOF exhibits threefold symmetry with respect to the center of the pore, resulting in inequivalent vertices of the network, which in turn influences their electronic properties (see Sec. III D). The proposed structural models are based on the results from low energy electron diffraction (LEED) [58], XPS, and XSW measurements, as well as from computed core-level shifts from DFT calculations.

The two components in the N1*s* XPS spectrum [Fig. 3(c)] for the mobile phase provided evidence for the existence of two different chemical environments of the N atoms. These peaks are assigned to the amine and imine groups of DPDI exhibiting an energy difference of 1.8 eV. Based on DFT modeling [Fig. 3(b)] [59], the peak at lower binding energy (397.6 eV) is assigned to the NH group, while the peak at higher binding energy (399.4 eV) is assigned to the NH_2 group. The energy difference between the NH_2 and NH peak was computed to be 1.86 eV, in very good agreement with

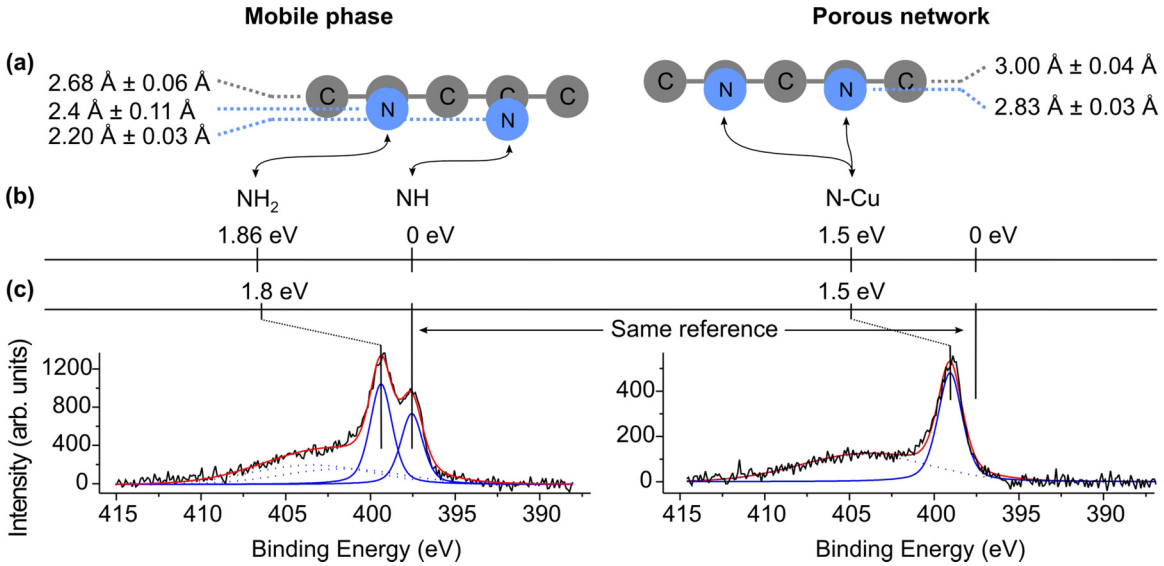

FIG. 3. (Color online) (a) Graphical illustration of the XSW results showing the adsorption heights of carbon and nitrogen atoms of DPDI in the mobile phase before annealing and of 3deh-DPDI in the porous network after annealing [59]. (b) Calculated core-level shifts of the nitrogen atoms with respect to the imine nitrogen of isolated DPDI adsorbed on Cu(111). (c) XPS spectra of the N1*s* core level together with the experimentally determined chemical shifts with respect to the imine nitrogen in the mobile phase. The spectra are shown after background subtraction. For the mobile phase, two peaks are visible at 397.6 and 399.4 eV, and for the porous network one peak is visible at 399.1 eV.

the experimentally obtained value (1.8 eV). In the case of the porous network, only one N1*s* component was found by XPS, with a chemical shift of 1.5 eV with respect to the NH peak of the mobile phase [Fig. 3(c)]. This chemical shift is reproduced by DFT only if Cu coordination of the 3deh-DPDI molecules is included in the model [Fig. 3(b)]. Other structures that we investigated failed to reproduce the experimentally observed value [59].

The surface distances of both the mobile phase and the MOF shown in Fig. 3(a) are the results of the XSW measurements. They led us to conclude that in the mobile phase the molecules interact mainly through their amine and imine groups (heights of 2.2 and 2.4 Å, respectively) with the Cu surface, while the carbon backbone is located considerably further away (average value of 2.68 Å), resulting in a substantially bent molecular structure.

For the surface network, the molecular adsorption height is generally larger than for the mobile phase. The nitrogen and carbon atoms reside at heights of 2.83 and 3.00 Å, respectively, above the substrate. These values are comparable to the sum of the respective vdW radii of nitrogen/carbon and copper [60]. Thus, it can be concluded that there is no direct chemical interaction between the molecules and the Cu surface. Instead, the chemical bonding within the network is mediated by Cu adatoms, which are responsible for the *decoupling of the molecules from the surface*. In contrast to the adsorbed network, where the Cu adatoms are positioned below the plane spanned by the organic exoligands and thus closer to the surface, the freestanding network with no Cu substrate was found to be completely planar in the DFT modeling. Therefore, the planar geometry of the coordination network is disrupted as a consequence of the interaction with the surface.

As discussed above, we found that the molecular adsorption height increases upon formation of the 2D MOF from the mobile phase. This observation is attributed to the local interactions between nitrogen atoms and Cu adatoms, resulting in the lifting of the molecule, including the perylene core, from the surface. For the related perylene derivative PTCDA (3,4,9,10-perylene-tetracarboxylic-dianhydride) adsorbed on Ag(111), a similar effect has been observed previously [19]. The molecule-substrate bonding distances in the disordered low temperature phase were found to be smaller compared to the well-ordered hydrogen-bonded herringbone structure formed at room temperature. Thus, increasing intermolecular interactions seem to result in decreasing molecule-surface interactions. In our case the perylene core is lifted by 0.32 Å, whereas the perylene core of PTCDA is lifted by only 0.06 Å. This large increase in adsorbate-substrate distance reported in this work indicates a fundamental change of the adsorbate-substrate interaction mechanism, which is attributed to the coordination between nitrogen and Cu adatoms, which mediate the intermolecular interactions as well as the bonding between the molecules and the substrate.

The interpretation is further supported by comparison with adsorbed diindenoperylene (DIP), a perylene derivative featuring no functional chemical groups available for metal coordination. The DIP molecule has an adsorption height of 2.59 Å on Cu(111) [61], which is in much closer agreement with the carbon adsorption height of the mobile DPDI phase than for the 2D MOF of 3deh-DPDI.

C. Description of adsorption heights by density functional theory

Our experimental measurements give detailed information on the (vertical) adsorption of molecules in 2D MOFs on surfaces and provide a benchmark, against which the accuracy of various density functionals can be tested. The experimental adsorption heights of both isolated DPDI molecules and 3deh-DPDI molecules in the 2D-MOF are compared in

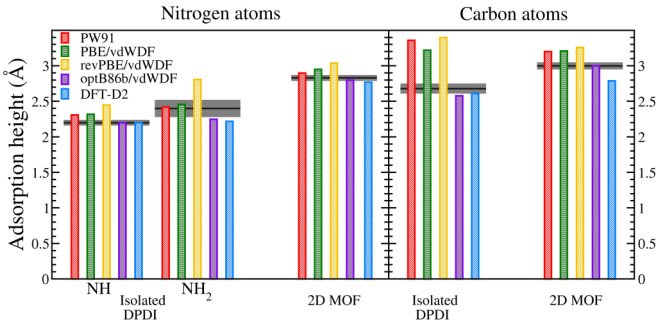

FIG. 4. (Color online) The graphical illustration summarizes the adsorption heights of the N atoms (left) as well as the average adsorption heights of the C atoms (right) for isolated DPDI (mobile phase) and 3deh-DPDI (2D MOF), respectively. The horizontal black lines show the experimentally derived values with the error margins, as indicated by the gray areas. The calculated values were obtained with noncorrected DFT (PW91), with three flavors of the van der Waals density functional (PBE/vdWDF, revPBE/vdWDF, optB86b/vdWDF) and with the Grimme correction (DFT-D2).

Fig. 4 to the calculated values obtained at different levels of theory, in particular addressing the way vdW interactions affect the adsorption heights. For the latter, we consider the semiempirical van der Waals-corrected DFT by Grimme (DFT-D2) as well as three flavors of the van der Waals density functional (vdWDF): revPBE/vdWDF, PBE/vdWDF, and optB86b/vdWDF.

Generally speaking, the adsorption heights for the nitrogen atoms are well described by the semilocal PW91 functional without vdW corrections and the vdW corrected functionals give essentially no systematic improvement. The PW91 functional gives a mean absolute error (MAE) of (0.07 ± 0.06) Å and the optB86b/vdWDF gives the overall best agreement with the experiments, with a marginally improved MAE of (0.06 ± 0.06) Å. These results suggest that inclusion of vdW interactions is not necessary for the description of the bonding of the N atoms to the Cu surface, neither for the isolated DPDI molecules nor for the 2D MOF.

The perylene core is found at a larger distance from the Cu surface than the N atoms for both the mobile phase and the 2D MOF. In particular, the noncorrected PW91 functional overestimates the adsorption heights of the carbon atoms (Fig. 4), making it crucial to include vdW interactions when modeling the adsorption heights of these atoms. These results will now be discussed for two bonding scenarios: isolated DPDI molecules, where the C atoms are relatively close to the Cu surface, and the 2D MOF, where the C atoms are further away from the surface.

For the isolated adsorbed molecules, the noncorrected PW91 functional severely overestimates the adsorption heights of the C atoms by almost 0.7 Å. In this case, DFT-D2 gives a slightly better agreement with the XSW data than optB86b/vdWDF, which in turn gives the best results among the vdWDFs. Both methods marginally underestimate the height by about 0.1 Å. In contrast to the isolated molecules, the adsorption height of the 2D MOF is best described by the optB86b/vdWDF, which yields a perfect agreement with the experiments. In this case, DFT-D2 underestimates the height by roughly the same magnitude as it is overestimated without the vdW correction.

Overall, it is found that optB86b/vdWDF gives the best agreement with the XSW experiments, with a MAE of (0.05 ± 0.05) Å for the carbon atoms, quite significantly smaller than the MAE of (0.14 ± 0.05) Å for DFT-D2. These values should be compared to the corresponding MAE of the noncorrected PW91 of (0.44 ± 0.05) Å. Thus, both methods provide a clear improvement compared to the noncorrected results, with optB86b/vdWDF reducing the MAE by one order of magnitude. Remarkably, this method is able to describe, with high accuracy, the adsorption height for both types of bonding scenarios, although DFT-D2 gives marginally better results for the isolated molecule. Recently, optB86b/vdWDF was illustrated to provide accurate adsorption heights both for other molecules and surfaces [62,63]. Until more high-level methods, such as the random phase approximation [64,65], become computationally feasible, the optB86b/vdWDF thus appears to be highly suitable for systems related to those presented here.

D. Symmetry properties identified by the STM fingerprint

The Cu adatoms, incorporated as metal centers in the 2D MOF, could not be directly imaged in the STM experiments at any tunneling conditions [Fig. 5(a)]. However, for large bias voltages (around 3 V) the molecules are no longer imaged. Instead, a characteristic protrusion appears at the location of the vertices—the region where the adatoms are located [Figs. 5(b) and 5(c)]. The same effect was observed for the 2D MOF made up from the related poly-N-heterocycle TAPP (1,3,8,10-tetraazaperopyrene) and Cu adatoms on Cu(111) [66]. The reason for this characteristic electronic feature—STM fingerprint—at high bias is in both cases an unoccupied electronic state, which is caused by the coordination of the organic ligands to the Cu adatoms. For a bias voltage of 2.9 V [Fig. 5(c)], the protrusions above the vertices exhibit two slightly different contrasts. The line scans in Fig. 5(d) illustrate this behavior for bias voltages between 2.5 and 3.4 V. The bright and dim protrusions are arranged in an alternating manner, indicating that the MOF contains two nonequivalent crossings, which is a signature of reduced rotational symmetry of the network.

The STM images taken at "normal" bias voltages suggest a sixfold rotational symmetry with respect to the pore center, corresponding to an on top position [Fig. 6(a)]. In this case, the three Cu adatoms are symmetrically arranged around a threefold hollow site, and all vertices are identical. The adsorption positions of the adatoms are close to top sites. However, with this arrangement the slightly different contrasts of adjacent protrusions in Figs. 5(c)) and 5(d) cannot be explained. By way of a lateral translation of the MOF, an isomeric structure is obtained, featuring two structurally different vertices [Fig. 6(b)]. Now, the Cu adatoms are symmetrically arranged around either a threefold hollow site or a Cu atom [labeled *A* and *B* vertex in Fig. 6(b)].

The network is threefold symmetric with respect to the center of the pore, which is now a threefold hollow site. Using this configuration, the STM images shown in Figs. 5(e)–5(g)

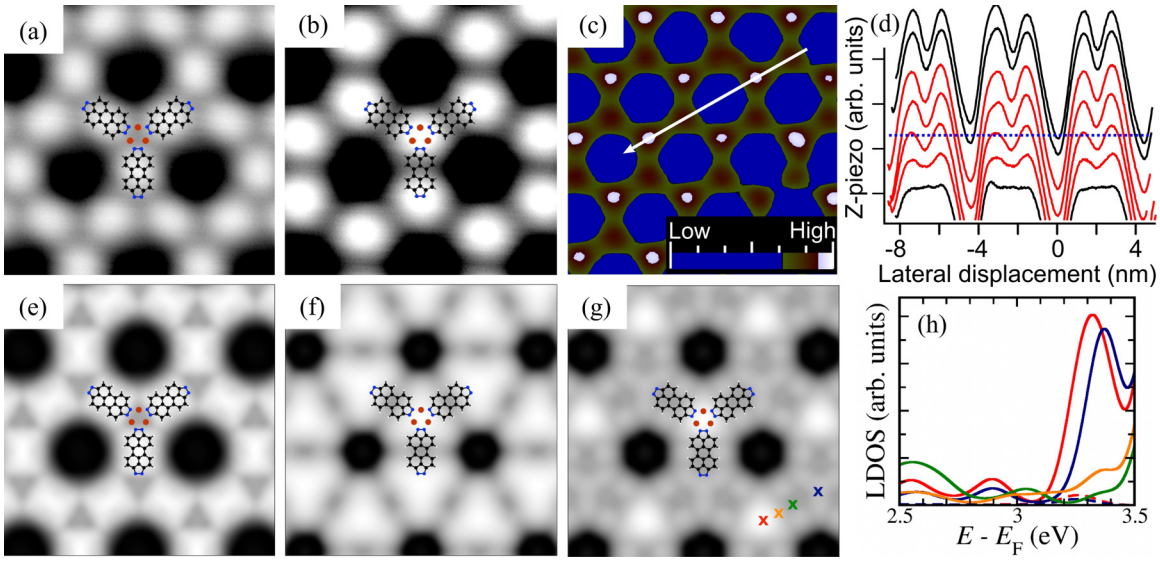

FIG. 5. (Color online) (a)–(c) Bias-dependent STM images (5×5 nm^2 for (a) and (b), 8×8 nm^2 for (c), 5 K) of the same area of the porous network illustrating that for "normal" bias voltages [(a) 1.5 V] the molecules are imaged while for large bias voltages [(b) 3.4 V and (c) 2.9 V] bright protrusions centered above the vertices of the network appear, where three adatoms are located. These protrusions are fingerprints for the presence of adatoms [66]. The false color code used in (c) helps to distinguish between the geometrically inequivalent vertices (see also Fig. 6). (d) The bias dependence of the apparent height of the two different vertices is reflected in the line scan (from bottom to top: 2.5, 2.7, 2.9, 3.1, 3.2, 3.3, 3.4 V), taken along the white arrow in (c). (e)–(g) In the simulated STM images, the LDOS was integrated from the Fermi level to the respective energies. As for the experimental images, for normal bias voltages [(e) $E_F + 1.5$ eV] the molecules are imaged while for large bias voltages the STM fingerprint for metal coordination is found [(f) $E_F + 3.4$ eV]. For an intermediate energy [(g) $E_F + 3.3$ eV], only every second vertex is apparent. (h) LDOS as a function of energy at four lateral positions as indicated by crosses in (g), showing that the fingerprint appears at two different energies for the geometrically different vertices (compare red and blue curves).

were simulated. They corroborate the experimental observations, especially the STM fingerprint very well, although a sharper transition is found in its energy dependence than in the experiments. Importantly, the simulated STM image at $E_F + 3.3$ eV [Fig. 5(g)] reproduces the bright and dim appearance of the vertices. When looking at the local density of states (LDOS) at different positions within the network [Figs. 5(g) and 5(h)], the reason for the observed effect becomes apparent. Only at the positions of the vertices, where the adatoms are located, dominant electron resonances are found [Fig. 5(h)].

Furthermore, the resonances for the vertices with the bright and dim signatures in Fig. 5(g) are found at slightly different energy values (3.3 vs 3.4 eV) explaining their different appearances in the STM images. In addition to verifying the presence of Cu adatoms, the STM fingerprint also provides experimental evidence that the network has a lower rotational symmetry than initially expected from topographical images.

The DFT calculations show that the adatoms in the threefold symmetric network adsorb closer to the energetically favorable hollow sites than in the sixfold symmetric network,

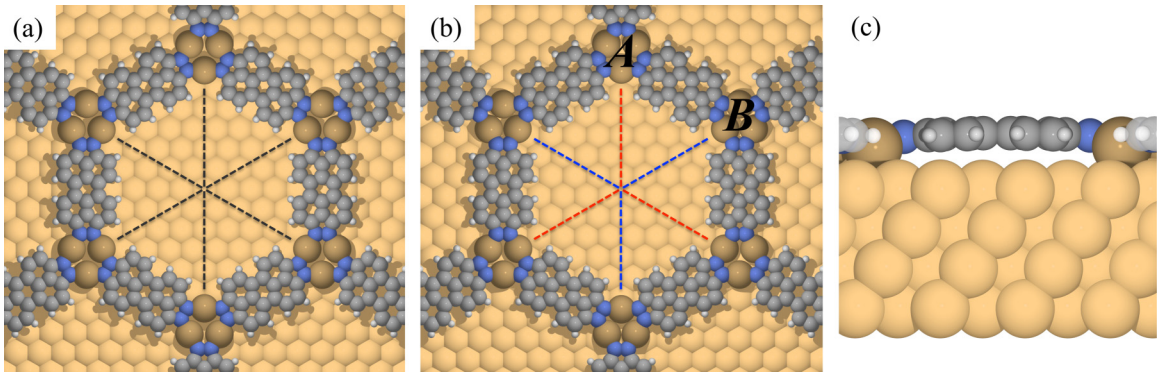

FIG. 6. (Color online) Isomeric adsorption structures of the 3deh-DPDI network coordinated to Cu adatoms, with binding energies of (a) 3.96 eV molecule^{-1} and (b) 4.27 eV molecule^{-1}. (a) For each vertex, the Cu adatoms adsorb on equivalent adsorption sites, resulting in a sixfold rotational symmetry of the pore (indicated by the black dashed lines). (b) A threefold rotational symmetry is obtained by a lateral translation of the network with respect to the Cu surface. Now, the red and blue dashed lines are not equivalent since the rotational center is a hollow site. This results in two different vertices for each surface unit cell (denoted A and B) with the adatoms adsorbed in energetically favorable hollow sites. (c) Side view of an adsorbed molecule in the asymmetric network.

making it more stable by 0.31 eV per molecule (3.96 vs 4.27 eV molecule^{-1} for the sixfold and the threefold symmetric network, respectively). The inequivalence of the *A* and *B* vertices leads to a calculated core-level shift (CLS) of 50 meV of the N1*s* peaks depending on whether the N atoms are participating in an *A* or a *B* vertex. However, this chemical shift is too small to be detected in XPS experiments. It should be noted that the energy difference between the two resonance positions is in perfect agreement with the simulated CLS for the nitrogen atoms in the *A* and *B* vertex, indicating that this is a local electrostatic effect.

IV. CONCLUSION

In conclusion, the determination of the molecule-substrate bonding distances has provided crucial information on a 2D MOF synthesized on a metal surface. As a model system we used the 2D MOF formed from the perylene derivative 3deh-DPDI on Cu(111) and compared it to its parent molecule DPDI. We find that as a result of the metal coordination, the molecule-substrate interaction is decreased and the molecules are essentially decoupled from the Cu(111) surface. Both the intermolecular interactions and the interactions between molecule and surface are mediated by the Cu adatoms, while the molecules reside at adsorption heights above the surface that are typical for physisorption. Experimental evidence for the incorporation of Cu adatoms in the network was provided by performing STM at large bias voltages of around 3 V. This so-called STM fingerprint of the N-Cu adatom coordination can even be used as a local spectroscopic tool, since it may reveal detailed structural anisotropies that are not identified by conventional spectroscopic techniques. We believe that our findings are largely generic for the behavior of MOFs on surfaces, also in case of other ligands and metal atoms. The incorporation of van der Waals interactions in theoretical modeling is essential for describing the adsorption heights of the molecules on surfaces. The optB86b/vdWDF method provides results in very good agreement with the XSW measurement, describing the relatively small adsorption height of the isolated molecule, as well as the lifting and decoupling of the molecules from the surface after the formation of the 2D MOF. This appears to be an appropriate method for the modeling of similar types of systems.

ACKNOWLEDGMENTS

We thank A. Scheybal for experimental support at the ESRF and S. Sellner for helpful discussions. This work was financially supported by the European Union through the Marie Curie Research Training Network PRAIRIES (MRTN_CT_2006-035810), by the Swiss National Science Foundation, the National Center of Competence in Research (NCCR) "Nanoscience," by the Foundation for Fundamental Research on Matter (FOM), by the Netherlands Organization for Scientific Research NWO (Chemical Sciences, VIDI Grant No. 700.10.424), the University of Heidelberg, and by the European Research Council (ERC-2012-StG 307760). Computer resources were allocated at the University of Liverpool and at the National Supercomputer Centre of Sweden through SNAC.

[1] O. M. Yaghi, M. O'Keeffe, N. W. Ockwig, H. K. Chae, M. Eddaoudi, and J. Kim, Nature (London) **423**, 705 (2003).
[2] S. Kitagawa, R. Kitaura, and S. Noro, Angew. Chem. Int. Ed. **43**, 2334 (2004).
[3] O. K. Farha and J. T. Hupp, Acc. Chem. Res. **43**, 1166 (2010).
[4] H. Furukawa, K. E. Cordova, M. O'Keeffe, and O. M. Yaghi, Science **341**, 1230444 (2013).
[5] J. V. Barth, Surf. Sci. **603**, 1533 (2009).
[6] N. Lin, S. Stepanow, M. Ruben, and J. V. Barth, Top. Curr. Chem. **287**, 1 (2009).
[7] S. Stepanow, N. Lin, and J. V. Barth, J. Phys.: Condens. Matter **20**, 184002 (2008).
[8] H. Spillmann, A. Dmitriev, N. Lin, P. Messina, J. V. Barth, and K. Kern, J. Am. Chem. Soc. **125**, 10725 (2003).
[9] S. Stepanow, M. Lingenfelder, A. Dmitriev, H. Spillmann, E. Delvigne, N. Lin, X. Deng, C. Cai, J. V. Barth, and K. Kern, Nat. Mater. **3**, 229 (2004).
[10] U. Schlickum, R. Decker, F. Klappenberger, G. Zoppellaro, S. Klyatskaya, M. Ruben, I. Silanes, A. Arnau, K. Kern, H. Brune, and J. V. Barth, Nano Lett. **7**, 3813 (2007).
[11] P. Gambardella, S. Stepanow, A. Dmitriev, J. Honolka, F. M. F. de Groot, M. Lingenfelder, S. S. Gupta, D. D. Sarma, P. Bencok, S. Stanescu, S. Clair, S. Pons, N. Lin, A. P. Seitsonen, H. Brune, J. V. Barth, and K. Kern, Nat. Mater. **8**, 189 (2009).
[12] Y. Li, J. Xiao, T. E. Shubina, M. Chen, Z. Shi, M. Schmid, H.-P. Steinrück, J. M. Gottfried, and N. Lin, J. Am. Chem. Soc. **134**, 6401 (2012).
[13] T. Sirtl, S. Schlögl, A. Rastgoo-Lahrood, J. Jelic, S. Neogi, M. Schmittel, W. M. Heckl, K. Reuter, and M. Lackinger, J. Am. Chem. Soc. **135**, 691 (2013).
[14] A. Saywell, W. Gren, G. Franc, A. Gourdon, X. Bouju, and L. Grill, J. Phys. Chem. C **118**, 1719 (2014).
[15] L. Kilian, A. Hauschild, R. Tmirov, S. Soubatch, A. Schöll, A. Bendounan, F. Reinert, T.-L. Lee, F. S. Tautz, M. Sokolowski, and E. Umbach, Phys. Rev. Lett. **100**, 136103 (2008).
[16] B. Schuler, W. Liu, A. Tkatchenko, N. Moll, G. Meyer, A. Mistry, D. Fox, and L. Gross, Phys. Rev. Lett. **111**, 106103 (2013).
[17] G. Mercurio, E. R. McNellis, I. Martin, S. Hagen, F. Leyssner, S. Soubatch, J. Meyer, M. Wolf, P. Tegeder, F. S. Tautz, and K. Reuter, Phys. Rev. Lett. **104**, 036102 (2010).
[18] A. Gerlach, F. Schreiber, S. Sellner, H. Dosch, I. A. Vartanyants, B. C. C. Cowie, T. Lee, and J. Zegenhagen, Phys. Rev. B **71**, 205425 (2005).
[19] A. Hauschild, R. Temirov, S. Soubatch, O. Bauer, A. Schöll, B. C. C. Cowie, T.-L. Lee, F. S. Tautz, and M. Sokolowski, Phys. Rev. B **81**, 125432 (2010).
[20] A. Gerlach, S. Sellner, F. Schreiber, N. Koch, and J. Zegenhagen, Phys. Rev. B **75**, 045401 (2007).

[21] N. Koch, A. Gerlach, S. Duhm, H. Glowatzki, G. Heimel, A. Vollmer, Y. Sakamoto, T. Suzuki, J. Zegenhagen, J. P. Rabe, and F. Schreiber, J. Am. Chem. Soc. **130**, 7300 (2008).

[22] O. Bauer, G. Mercurio, M. Willenbockel, W. Reckien, C. H. Schmitz, B. Fiedler, S. Soubatch, T. Bredow, F. S. Tautz, and M. Sokolowski, Phys. Rev. B **86**, 235431 (2012).

[23] I. Kröger, P. Bayerdorfer, B. Stadtmüller, C. Kleimann, G. Mercurio, F. Reinert, and C. Kumpf, Phys. Rev. B **86**, 195412 (2012).

[24] G. Mercurio, O. Bauer, M. Willenbockel, N. Fairley, W. Reckien, C. H. Schmitz, B. Fiedler, S. Soubatch, T. Bredow, M. Sokolowski, and F. S. Tautz, Phys. Rev. B **87**, 045421 (2013).

[25] B. Stadtmüller, S. Schröder, F. B. Bocquet, C. Henneke, C. Kleimann, S. Soubatch, M. Willenbockel, B. Detlefs, J. Zegenhagen, T.-L. Lee, F. S. Tautz, and C. Kumpf, Phys. Rev. B **89**, 161407(R) (2014).

[26] E. Goiri, M. Matena, A. El-Sayed, J. Lobo-Checa, P. Borghetti, C. Rogero, B. Detlefs, J. Duvernay, J. E. Ortega, and D. G. de Oteyza, Phys. Rev. Lett. **112**, 117602 (2014).

[27] T.-C. Tseng, C. Lin, X. Shi, S. L. Tait, X. Liu, U. Starke, N. Lin, R. Zhang, C. Minot, M. A. van Hove, J. I. Cerdá, and K. Kern, Phys. Rev. B **80**, 155458 (2009).

[28] X. Q. Shi, C. Lin, C. Minot, T.-C. Tseng, S. L. Tait, N. Lin, R. Q. Zhang, K. Kern, J. I. Cerda, and M. A. Van Hove, J. Phys. Chem. C **114**, 17197 (2010).

[29] N. Abdurakhmanova, A. Floris, T.-C. Tseng, A. Comisso, S. Stepanow, A. De Vita, and K. Kern, Nat. Commun. **3**, 940 (2012).

[30] A. Tkatchenko, L. Romaner, O. T. Hofmann, E. Zojer, C. Ambrosch-Draxl, and M. Scheffler, MRS Bull. **35**, 435 (2010).

[31] T. Sirtl, J. Jelic, J. Meyer, K. Das, W. M. Heckl, W. Moritz, J. Rundgren, M. Schmittel, K. Reuter, and M. Lackinger, Phys. Chem. Chem. Phys. **15**, 11054 (2013).

[32] S. Grimme, J. Comp. Chem. **27**, 1787 (2006).

[33] A. Tkatchenko and M. Scheffler, Phys. Rev. Lett. **102**, 073005 (2009).

[34] V. Ruiz, W. Liu, E. Zojer, M. Scheffler, and A. Tkatchenko, Phys. Rev. Lett. **108**, 146103 (2012).

[35] W. Liu, A. Tkatchenko, and M. Scheffler, Acc. Chem. Res. (2014), doi:10.1021/ar500118y.

[36] J. Tao and A. M. Rappe, Phys. Rev. Lett. **112**, 106101 (2014).

[37] M. Dion, H. Rydberg, E. Schröder, D. C. Langreth, and B. I. Lundqvist, Phys. Rev. Lett. **92**, 246401 (2004).

[38] F. Hanke, M. S. Dyer, J. Björk, and M. Persson, J. Phys.: Condens. Matter **24**, 424217 (2012).

[39] J. Klimeš, D. R. Bowler, and A. Michaelides, Phys. Rev. B **83**, 195131 (2011).

[40] V. R. Cooper, Phys. Rev. B **81**, 161104 (2010).

[41] K. Lee, E. D. Murray, L. Kong, B. I. Lundqvist, and D. C. Langreth, Phys. Rev. B **82** 081101 (2010).

[42] I. Hamada, Phys. Rev. B **89**, 121103 (2014).

[43] A. Shchyrba, C. Wäckerlin, J. Nowakowski, S. Nowakowska, J. Björk, S. Fatayer, J. Girovsky, T. Nijs, S. C. Martens, A. Kleibert, M. Stöhr, N. Ballav, T. A. Jung, and L. H. Gade, J. Am. Chem. Soc. **136**, 9355 (2014).

[44] M. Stöhr, M. Wahl, C. H. Galka, T. Riehm, T. A. Jung, and L. H. Gade, Angew. Chem. Int. Ed. **44**, 7394 (2005).

[45] I. Horcas, R. Fernández, J. M. Gómez-Rodríguez, J. Colchero, J. Gómez-Herrero, and A. M. Baro, Rev. Sci. Instrum. **78**, 013705 (2007).

[46] G. Kresse and J. Furthmüller, Phys. Rev. B **54**, 11169 (1996).

[47] P. E. Blöchl, Phys. Rev. B **50**, 17953 (1994).

[48] G. Kresse and D. Joubert, Phys. Rev. B **59**, 1758 (1999).

[49] J. P. Perdew, J. A. Chevary, S. H. Vosko, K. A. Jackson, M. R. Pederson, D. J. Singh, and C. Fiolhais, Phys. Rev. B **46**, 6671 (1992).

[50] Y. Zhang and W. Yang, Phys. Rev. Lett. **80**, 890 (1998).

[51] J. P. Perdew, K. Burke, and M. Ernzerhof, Phys. Rev. Lett. **77**, 3865 (1996).

[52] E. R. McNellis, J. Meyer, and K. Reuter, Phys. Rev. B **80**, 205414 (2009).

[53] J. Tersoff and D. R. Hamann, Phys. Rev. Lett. **50**, 1998 (1983).

[54] N. Lorente and M. Persson, Faraday Discuss. **117**, 277 (2000).

[55] A monolayer of DPDI corresponds to the amount of molecules that is needed to cover the complete Cu surface, and amounts to 0.84 molecules/nm^2.

[56] W. Jaworek and F. Vögtle, F. Chem. Ber. **124**, 347 (1991).

[57] M. Matena, M. Stöhr, T. Riehm, J. Björk, S. Martens, M. S. Dyer, M. Persson, J. Lobo-Checa, K. Müller, M. Enache, H. Wadepohl, J. Zegenhagen, T. A. Jung, and L. H. Gade, Chem. Eur. J. **16**, 2079 (2010).

[58] The LEED measurements found a $p(10 \times 10)$ superstructure for the 2D MOF, see Ref. [44].

[59] See Supplemental Material at http://link.aps.org/supplemental/10.1103/PhysRevB.90.125408 for additional experimental and computational details.

[60] The vdW radii for C, N, and Cu are 1.7, 1.55, and 1.4 Å, respectively.

[61] C. Bürker, N. Ferri, A. Tkatchenko, A. Gerlach, J. Niederhause, T. Hosokai, S. Duhm, J. Zegenhagen, N. Koch, and F. Schreiber, Phys. Rev. B **87**, 165443 (2013).

[62] J. Björk and S. Stafström, ChemPhysChem. (2014), doi:10.1002/cphc.201402063.

[63] J. Carrasco, W. Liu, A. Michaelides, and A. Tkatchenko, J. Chem. Phys. **140**, 084704 (2014).

[64] J. Harl and G. Kresse, Phys. Rev. Lett. **103**, 056401 (2009).

[65] L. Schimka, J. Harl, A. Stroppa, A. Grüneis, M. Marsman, F. Mittendorfer, and G. Kresse, Nat. Mater. **9**, 741 (2009).

[66] J. Björk, M. Matena, M. S. Dyer, M. Enache, J. Lobo-Checa, L. H. Gade, T. A. Jung, M. Stöhr, and M. Persson, Phys. Chem. Chem. Phys. **12**, 8815 (2010).